JNS

CLINICAL ARTICLE

J Neurosurg 132:150–158, 2020

A novel robot-guided minimally invasive technique for brain tumor biopsies

Georgi Minchev, MD,[1] Gernot Kronreif, PhD,[2] Wolfgang Ptacek, DI(FH),[2] Christian Dorfer, MD,[1] Alexander Micko, MD, PhD,[1] Svenja Maschke, MD,[1] Federico G. Legnani, MD,[3] Georg Widhalm, MD, PhD,[1] Engelbert Knosp, MD,[1] and Stefan Wolfsberger, MD[1]

[1]Department of Neurosurgery, Medical University of Vienna; [2]Austrian Center of Medical Innovation and Technology (ACMIT), Wiener Neustadt, Austria; and [3]Department of Neurosurgery, Fondazione IRCCS Instituto degli Neurologica C. Besta, Milan, Italy

OBJECTIVE As decisions regarding tumor diagnosis and subsequent treatment are increasingly based on molecular pathology, the frequency of brain biopsies is increasing. Robotic devices overcome limitations of frame-based and frameless techniques in terms of accuracy and usability. The aim of the present study was to present a novel, minimally invasive, robot-guided biopsy technique and compare the results with those of standard burr hole biopsy.

METHODS A tubular minimally invasive instrument set was custom-designed for the iSYS-1 robot-guided biopsies. Feasibility, accuracy, duration, and outcome were compared in a consecutive series of 66 cases of robot-guided stereotactic biopsies between the minimally invasive (32 patients) and standard (34 patients) procedures.

RESULTS Application of the minimally invasive instrument set was feasible in all patients. Compared with the standard burr hole technique, accuracy was significantly higher both at entry (median 1.5 mm [range 0.2–3.2 mm] vs 1.7 mm [range 0.8–5.1 mm], p = 0.008) and at target (median 1.5 mm [range 0.4–3.4 mm] vs 2.0 mm [range 0.8–3.9 mm], p = 0.019). The incision-to-suture time was significantly shorter (median 30 minutes [range 15–50 minutes] vs 37.5 minutes [range 25–105 minutes], p < 0.001). The skin incision was significantly shorter (median 16.3 mm [range 12.7–23.4 mm] vs 28.4 mm [range 20–42.2 mm], p = 0.002). A diagnostic tissue sample was obtained in all cases.

CONCLUSIONS Application of the novel instrument set was feasible in all patients. According to the authors' data, the minimally invasive robot-guidance procedure can significantly improve accuracy, reduce operating time, and improve the cosmetic result of stereotactic biopsies.

https://thejns.org/doi/abs/10.3171/2018.8.JNS182096

KEYWORDS accuracy; biopsy; minimally invasive; robotic device; stereotaxy; oncology; surgical technique

As molecular pathology continues to emerge as the basis for many oncological treatment decisions,[23] the frequency of brain tumor biopsies is rising. For accurate tissue sampling with the least possible morbidity, high precision in stereotactic biopsies is essential.

If maximum accuracy is needed, e.g., in brainstem biopsies, skull-mounted stereotactic frames are still widely preferred.[26,33] The price of high-accuracy stereotactic frames, however, is a time-consuming, complex, and inconvenient procedural workflow and often restricted access to the surgical field.[3,4,10,12,13,28] Biopsies of large supratentorial lesions are commonly performed "frameless" with manual adjustment of a navigation-guided mechanical positioning device. However, these neurosurgical procedures are routinely performed with considerably lower accuracy.[1,2,13,28,29,33,34]

We recently presented a small form factor robot-guidance device that combines the advantages of frameless and frame-based techniques into a highly accurate, safe, and rapid stereotactic procedure.[27] However, this procedure

ABBREVIATIONS RTE = real target error; SEEG = stereo-electroencephalography.

SUBMITTED July 20, 2018. **ACCEPTED** August 28, 2018.
INCLUDE WHEN CITING Published online January 18, 2019; DOI: 10.3171/2018.8.JNS182096.

TABLE 1. Patient characteristics

	Standard Procedure	Minimally Invasive
No. of patients	34	32
F/M sex ratio	1:1.27	1.28:1
Median age, yrs (range)	50 (20–83)	56 (29–82)
Rt/lt side	1:1.12	1.28:1
Location		
Frontal	8	4
Temporal	7	7
Brainstem	6	2
Corpus callosum	2	8
Parietal/trigonal	3	3
Basal ganglia/thalamic	4	4
Central	3	1
Multiple	1	0
Cerebellar	0	3

TABLE 2. Histological diagnosis

	No. of Patients
Astrocytoma	16
Grade I (pilocytic)	1
Grade II	3
Grade III	12
Oligodendroglioma	4
Grade II	3
Grade III	1
GBM (grade IV)	25
Lymphoma	8
Germinoma	2
Glioma (isomorphic)	2
Metastasis	2
Multiple sclerosis plaque	1
Gliomatosis	1
Histiocytosis	1
Chondrosarcoma	1
Gliosarcoma	1
Medulloblastoma	1
Vasculitis	1

GBM = glioblastoma.

still required a considerable skin and muscle incision and a standard burr hole with its drawbacks. Furthermore, the lack of stable bone contact of the guidance device assembly could potentially reduce procedural accuracy.

To pursue the goal of minimal invasiveness and to increase the procedural accuracy at the same time, we adapted a tubular instrument set originally designed for stereo-electroencephalography (SEEG) depth electrode placement at our department[8,9] for robot-guided frameless stereotactic biopsies. For the skin incision, the presented technique requires a minimally invasive incision of the skin to rigidly fixate a stereotactic drill guide to the bone. For bone drilling, a stereotactic small twist drill hole of only 3.2 mm in diameter is necessary to accommodate a standard biopsy needle. We hypothesized that as the system attaches the robot to the skull, the resulting rigid system may increase accuracy. As the workflow is optimized and skin retraction, electrocautery, and drilling are reduced to a minimum, procedural duration may be reduced at the same time.

The aim of the present study was to evaluate the feasibility of a novel, minimally invasive biopsy technique and compare the results with a standard burr hole biopsy procedure performed with robotic guidance in terms of accuracy, procedural duration, and cosmetic result.

Methods

The study was approved by the ethics committee of the Medical University of Vienna and the Austrian Agency for Health and Food Safety.

Patients

Since development of the proposed technique commenced in October 2014, 66 consecutive robot-guided stereotactic biopsies were performed with either the minimally invasive instrument set (32 cases) or the standard burr hole procedure (34 patients) depending on the surgeon's preference (Tables 1 and 2).

All patients gave informed consent to their participation in the study.

Surgical Planning

The iSYS-1 robotic guidance device (iSYS Medizintechnik) was used for all biopsy procedures. It is a 4-axial modular positioning system that receives spatial data of the predefined trajectory and present instrument position from the navigation system (StealthStation S7, Medtronic) and precisely aligns the biopsy needle with the trajectory. The surgeon is in full control of advancing the needle manually to the target point. For a detailed description of the robotic guidance system, see our previous work.[27]

The biopsy target was defined 1) by significant contrast enhancement on MRI, or if absent 2) by highest tracer uptake on ^{11}C-PET scan, or if also absent 3) by a pathological hyperintense area on FLAIR/T2-weighted MRI.[30,37] The needle trajectory was defined on T1-weighted contrast-enhanced MR images as the shortest distance from an entry point behind the hairline to the target and adjusted to avoid eloquent cortex/fibers, vessels, sulci, or ventricles.

Patient registration was performed by optic tracking of CT data merged with MRI/PET either by surface match (350 surface points) or by point-to-point match of 6 bone-screw fiducials in cases of small or deep-seated lesions.

Surgical Workflow

All procedures were performed under general anesthesia with the patient rigidly held in a head clamp. The robot was mounted to the head clamp adapter ipsilateral to the lesion and contralateral to the navigation reference frame.

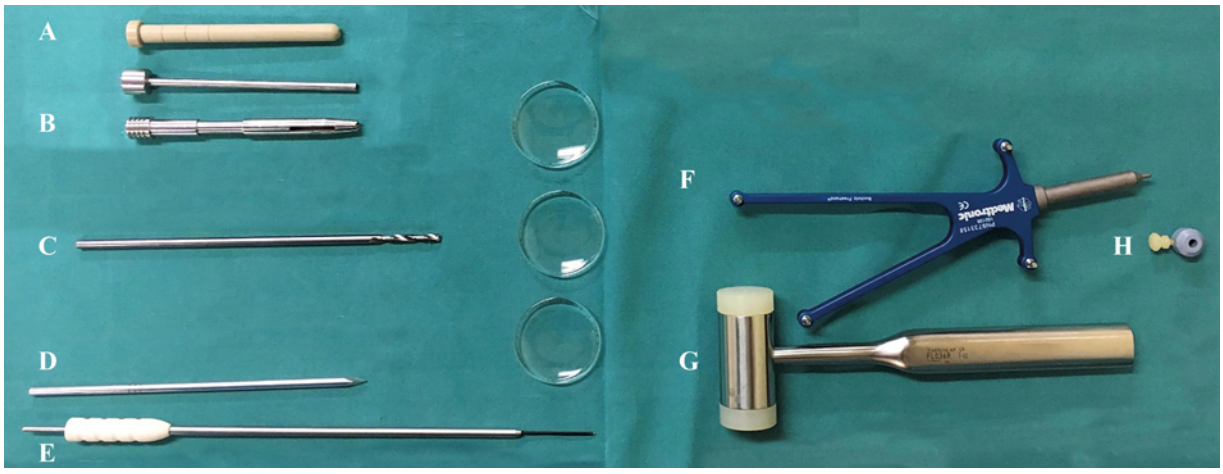

FIG. 1. Minimally invasive instrument set for robot-guided stereotactic brain biopsies (order of labeling does not correspond with the workflow). **A:** Spacer bit for prepositioning of the robotic device (upper bit) and reduction sheath for Nashold passive biopsy needle (lower bit). **B:** Custom-designed guidance sheath with special bone-anchor teeth for rigid bone contact. **C:** Twist drill bit (3.2-mm diameter) for the Colibri drill battery-driven system. **D:** K-wire (4-mm diameter) for percutaneous bone fixation. **E:** Monopolar needle for perforation and electrocautery of the dura and pia. **F:** Standard Vertek probe (Medtronic) for optical tracking and precise trajectory alignment. **G:** Hammer for bone fixation of K-wire and guidance sheath. **H:** Adjustable stop device for the monopolar needle and biopsy needle for depth control.

Sterile preparation and draping were performed in a standard fashion.

At the beginning of the procedure, the robot was manually prepositioned within 2 cm of the entry point and automatically aligned its guidance sheath with the preplanned trajectory.

Minimally Invasive Biopsy Procedure

First, a 4-mm stab incision of the skin was performed through the robotic guidance sheath. With the robot temporarily moved out of the surgical field by joystick control, this incision was then enlarged to a minimum length of 12.4 mm to accommodate the custom-designed guide tube with a diameter of 7.9 mm ($d \times \pi/2$).

After auto-realignment of the robot, the custom-designed guidance tube (10-cm length, 4-mm inner diameter, bone-anchor teeth at the distal end) was introduced through the robotic guidance sheath to the level of the skin. Then, a 4-mm K-wire was inserted through guidance tube and skin incision down to the level of the bone and affixed by slight pounding. The guidance tube was also advanced along the K-wire and affixed by pounding onto the bone and the K-wire was removed. At this point, a rigid connection of the robotic system to the skull was ensured.

Stereotactic drilling was performed through the guidance tube using a battery-driven system (Colibri Power Tools, Johnson & Johnson, Synthes) with a 3.2-mm-diameter drill with a stop device positioned at 10 cm plus thickness of the bone on individual CT. For perforation of the dura and pia, we performed coagulation with a monopolar needle through the drill hole. The instruments used in this procedure and the workflow are shown in Figs. 1 and 2, respectively.

Standard Burr Hole Biopsy Procedure

First, a skin mark was performed through the robotic guidance sheath. Then, the robot was temporarily moved out of the surgical space for the skin incision, electrocautery, and insertion of the retractor.

For bone drilling, the robot was automatically realigned, and a burr hole was drilled through the robotic guidance sheath using an 8-mm-diameter high-speed drill. Then, the robot was again temporarily moved out of the surgical space for completion of the burr hole approach by application of bone wax, dural coagulation, and cruciform dural opening.

For the actual biopsy procedure, a Nashold-type 2.1-mm-diameter biopsy needle was manually advanced through the guide tube to the target under continuous depth guidance by its 2 passive markers. Samples were taken as appropriate. Closure was performed by 1–2 skin sutures in the minimally invasive biopsy group, by placing a cube of Gelfoam into the burr hole and double-layered suturing in the standard burr hole group.

Accuracy

Intraoperative Accuracy Assessment

The registration accuracy was checked on anatomical landmarks[38] and repeated if judged inaccurate. The trajectory alignment error, a parameter for deviation between instrument and trajectory, was continuously updated by the navigation system until locked for biopsy needle advancement.

Postoperative Accuracy Assessment

The real target error (RTE), a parameter that defines how accurately a procedure has reached the target, was assessed by merging the postoperative (within 48 hours) CT or MR images with the preoperative planning images using the same scanner. The RTE of a navigation-guided stereotactic procedure is derived from multiple factors,

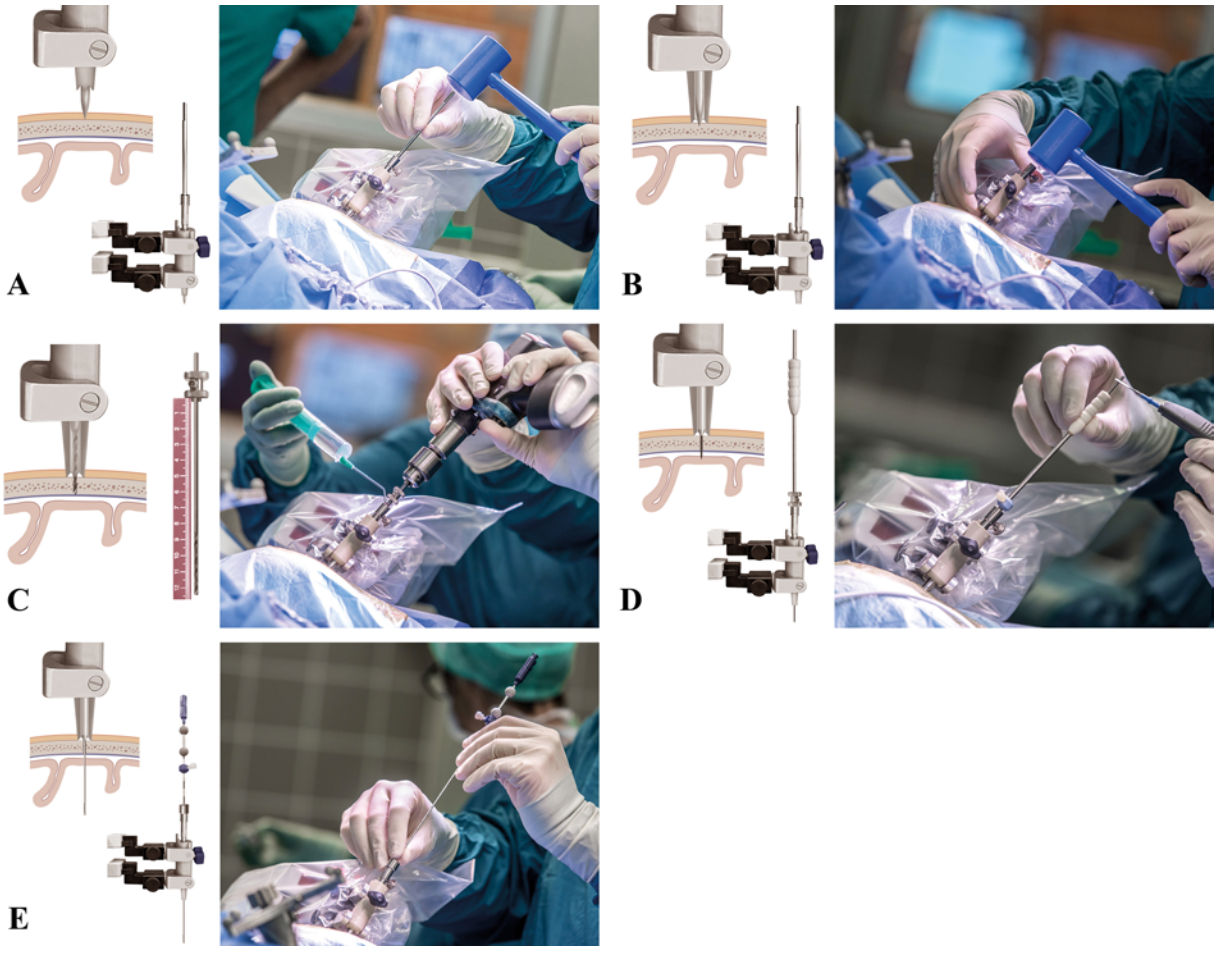

FIG. 2. Workflow of the novel minimally invasive instrument set (schematic, *left column*; intraoperative, *right column*). After trajectory alignment and stab incision, the K-wire is affixed onto the external table of the skull bone (**A**) by gentle punching through the guidance sheath. The custom-designed guidance sheath is then advanced along the K-wire, and its bone-anchor teeth are fixated onto the bone, ensuring a rigid connection to the patient's head (**B**). Stereotactic drilling is performed through the guidance tube using a 3.2-mm-diameter drill bit with a stop device positioned at 10 cm plus thickness of the bone (**C**). A monopolar needle with a prepositioned depth stop device is used for perforation and coagulation of the dura and pia (**D**). For tissue sampling, a Nashold-type 2.1-mm-diameter biopsy needle is manually advanced through the guidance sheath to the target under continuous depth guidance (**E**).

mainly from surface registration (< 2 mm),[15,25] distortion of imaging (0.23 ± 0.03 mm for CT with 1-mm slice thickness,[5] < 0.4 mm for MRI depending on field strength and static field inhomogeneities[24,35]), and technical system error (< 0.12 mm).[18] For the target point, this value was assessed by air bubbles and the biopsy cavity; for the entry point, the value was defined as the distance between the preplanned trajectory and the center of the burr or drill hole. Due to inaccuracy, PET data were excluded for accuracy assessment. We measured the maximum deviation at entry and target points in the x-/y-plane. Since the z-plane is not dependent on the technique but rather on the surgeon advancing the instrument and due to multiple samples taken along the preplanned trajectory at the target site, it was excluded for accuracy assessment. Due to the image resolution of < 1 mm of CT and MRI in the x-/y-plane, the navigation system's calculated resolution of 0.1 mm was suitable for our results.

Clinical Outcome

Diagnostic yield was calculated as the rate of representative samples as established by the local neuropathology team according to the WHO 2016 criteria.[23] Postoperative hemorrhage was classified according to the location (target site or along the trajectory) and size on early postoperative CT scanning. Procedure-related clinical status changes were assessed at discharge and at early postoperative follow-up and compared with the preoperative status.

Cosmetic Result

The length of the skin incision was manually measured on the 3D skin surface model of the early postoperative CT scans.

Statistical Analysis

For statistical analysis, IBM SPSS software (version

TABLE 3. Accuracy assessment

	Median (range)		
	Standard Procedure	Minimally Invasive Procedure	p Value*
Vol (cm^3)			
Lesion	9.45 (0.6–91.6)	9.3 (0.1–34.5)	NS
Target	2.65 (0.6–66.9)	7.3 (0.1–34.5)	NS
Accuracy, mm			
Intraop error (navigation)			
Trajectory alignment error	0.1 (0.0–0.1)	0.1 (0.0–0.1)	
Postop real error			
At entry	1.7 (0.8–5.1)	1.5 (0.2–3.2)	**0.008**
At target	2.0 (0.8–3.9)	1.5 (0.4–3.4)	**0.019**
Skin-to-suture procedural duration, mins	37.5 (25–105)	30 (15–50)	**<0.001**

NS = not significant.
Boldface type indicates statistical significance.
* Unpaired t-test.

22.0, IBM Corp.) was used. We compared median values of the standard burr hole and minimally invasive biopsy procedures using the unpaired t-test. Values are given as mean and standard deviation or median and range. A p value of < 0.05 was considered significant.

Results

Feasibility

Overall, application of the robotic device was feasible in all 66 patients, i.e., conversion to manual stereotactic arm–based biopsy was never needed. In particular, application of the proposed minimally invasive instrument set for stereotactic biopsies proved feasible in all 32 patients, and conversion of the twist drill hole procedure to a burr hole procedure was never required.

Patient, Tumor, and Procedure Characteristics

The following targets were chosen for biopsy: contrast enhancement on MRI (n = 59), maximum tracer uptake on PET (n = 5), and FLAIR/T2 hyperintensity (n = 2). Patients were positioned supine in 53 cases and prone in 13 cases. Patient registration was performed by surface match (n = 57) or bone screws (n = 9) in cases of posterior fossa/brainstem or small deep-seated lesions.

There was no significant difference between the techniques in terms of lesion volume (minimally invasive group: median 9.3 cm^3 [range 0.1–34.5 cm^3] and standard burr hole group: median 9.45 cm^3 [range 0.6–91.6 cm^3], p = 0.323) or biopsy target volume (minimally invasive group: median 7.3 cm^3 [range 0.1–34.5 cm^3] and standard burr hole group: median 2.65 cm^3, range 0.1–66.9 cm^3, p = 0.674; Table 3).

Accuracy

Target alignment performed by the robotic system was accurate to ≤ 0.1 mm in all 66 cases.

The RTE is stratified by the registration method: using surface registration, the RTE was significantly less when using the novel minimally invasive technique than when using the standard burr hole technique both at entry points (median RTE minimally invasive group: 1.5 mm [range 0.2–3.2 mm] vs standard burr hole group: 1.7 mm [range 0.8–5.1 mm], p = 0.008) and at target points (median RTE minimally invasive group: 1.5 mm [range 0.4–3.4 mm] vs standard burr hole group: 2.0 mm [range 0.8–3.9 mm], p = 0.019; Table 3).

In the 7 cases of bone-screw registration in the minimally invasive biopsy group, further improvement in accuracy did not reach significance. At entry points, the median RTE was 1.2 mm (range 0.2–2.5 mm) for bone screws versus 1.5 mm (range 0.4–3.2 mm) for surface registration, and at target points, the median RTE was 1.6 mm (range 0.6–2.7 mm) for bone screws versus 1.5 mm (range 0.4–3.4 mm) for surface registration.

Procedural Time

Procedural duration assessed by incision-suture time was significantly shorter using the novel minimally invasive technique than the standard burr hole technique (minimally invasive group: median duration 30 minutes [range 15–50 minutes] vs standard burr hole group: 37.5 minutes [range 25–105 minutes], p < 0.001; Table 3).

Clinical Outcome

Diagnostic Yield

A diagnostic tissue sample was obtained in all cases. In 1 patient, histopathological workup of the sample (taken precisely from the target point as confirmed on postoperative imaging) revealed unspecific tissue alterations (see Fig. 3D–F). This histological result was later confirmed by open resection.

Early Postoperative Hemorrhage

No intracerebral hemorrhage was detected along the trajectory, and no epi- or subdural hemorrhage was observed in any patient in the minimally invasive group. An intralesional hemorrhage at the target position was observed on early postoperative CT scanning in 1 patient in the standard burr hole group (2.9%, 38-mm diameter).

This patient experienced transient hemiparesis and speech disturbance, but recovered to the preoperative neurological state until discharge.

Cosmetic Result

The skin incision was significantly smaller with the minimally invasive technique than with the standard burr hole technique (median length in the minimally invasive group: 16.3 mm [range 12.7–23.4 mm] vs standard burr hole group: 28.4 mm [range 20–42.2 mm], $p = 0.002$). We did not observe wound healing complications due to forced dilation or infection in any case.

Discussion

Despite advances in imaging, tumor diagnosis and treatment decisions are increasingly based on molecular markers obtained from brain tumor biopsies. Therefore, accurate tissue sampling and high precision of stereotactic biopsies with low morbidity is essential. We previously presented a novel miniature robot system for stereotactic interventions and demonstrated its high procedural accuracy and straightforward workflow.[8,27] To further pursue the goals of high accuracy and minimal invasiveness, we adapted the tubular instrument set originally designed for placement of SEEG depth electrodes[8] to stereotactic biopsy procedures, and in this report we compared this novel minimally invasive biopsy technique with the standard burr hole technique in a consecutive series of 66 patients.

Feasibility

Application of the novel minimally invasive instrument set was feasible in all cases with a short learning curve. Even trajectories to "extreme" locations (e.g., low temporal, posterior fossa) and at extreme angles were possible with the novel instrument set.

Approaches toward minimizing invasiveness for frameless stereotactic brain tumor biopsies have been made before. For example, the skull-mounted Navigus (Medtronic) passive biopsy system has been used for stereotactic biopsies.[31] Due to the screw fixation of the base onto the bone, high system stability could be achieved at the cost of a more invasive procedure with a larger burr hole and large skin incision. To our knowledge, there are no reports of procedural accuracy in a clinical setting using this system.

Accuracy

The RTE of a navigation-guided stereotactic procedure is derived from the technical or system inherent error, the registration error, and the mechanical alignment error.[11,15,16,24,25,32,35] The proposed innovation aims to improve the mechanical alignment errors; current arm-based biopsy systems suffer an inherent instability due to the lack of direct contact between the mechanical arm and bony skull. Through stable bone contact, our custom-designed guidance tube closes the mechanical loop (skull clamp—patient's head—guidance tube—robotic device—skull clamp). This may explain the higher accuracy at entry and target points in the minimally invasive group than in the standard burr hole group. Therefore, our novel, minimally invasive method can reduce the RTE to the system and registration errors. Accuracy results of previous reports compare well with the results of our trial using surface registration.[21,22,36]

Cosmetic Result

Skin incisions for burr hole biopsies are usually performed freehand, with the length of the incision increasing relative to the thickness of the skin-muscle layer. With electrocautery, periosteal elevation, and retractor insertion, trauma to the skin-muscle layer can be considerable.

The advantage of the presented minimally invasive technique is the precise placement of a stereotactic stab incision at a length unaffected by the thickness of the skin-muscle layer (Fig. 3). This was found especially important in areas of thick muscle, such as for temporopolar and posterior fossa trajectories. Due to the significantly shorter incision, surgical trauma was minimized and the cosmetic result improved.

Procedural Duration

The operating room time of a stereotactic biopsy procedure is based on setup time, sampling time, and time for intraoperative tissue diagnosis. While the latter can be reduced by application of exogenous fluorophores,[37] setup time was already reduced by application of the robotic device.[27]

The application of the proposed minimally invasive technique aimed to reduce sampling time. Despite its large size of approximately 8 mm diameter, standard burr holes for biopsies not uncommonly require further bone adjustments if performed freehand. This was not the case in our standard burr hole group as drilling was performed with stereotactic guidance. However, the robotic guidance device still needed to be pivoted away into its park position for bone waxing, coagulation, and incision of the dura.

For our minimally invasive technique, the following improvements in stereotactic drilling were introduced. First, to keep the drill head centered and prevent sliding on the external table of the skull, a small divot was punched with the K-wire as mentioned above. Furthermore, the drill head diameter was optimized to 3.2 mm so that the resulting twist drill hole could easily accommodate the biopsy needle without burr resistance and consequently without loss of haptic feedback from intracranial structures.

Safety

The proposed instrument set does not interfere with robotic alignment movement. Robotic movements are only possible in the x and y directions by continuously pressing a dead man's switch and for security reasons. Inadvertent robotic movements without the surgeon's interaction are therefore not possible. The surgeon remains in control of the instrument insertion into the cranium at all times.

Complications

Wound Healing

After stereotactic skin incision and enlargement, we mechanically dilated the skin incision using the custom-made guidance tube. Despite this small blunt trauma, no

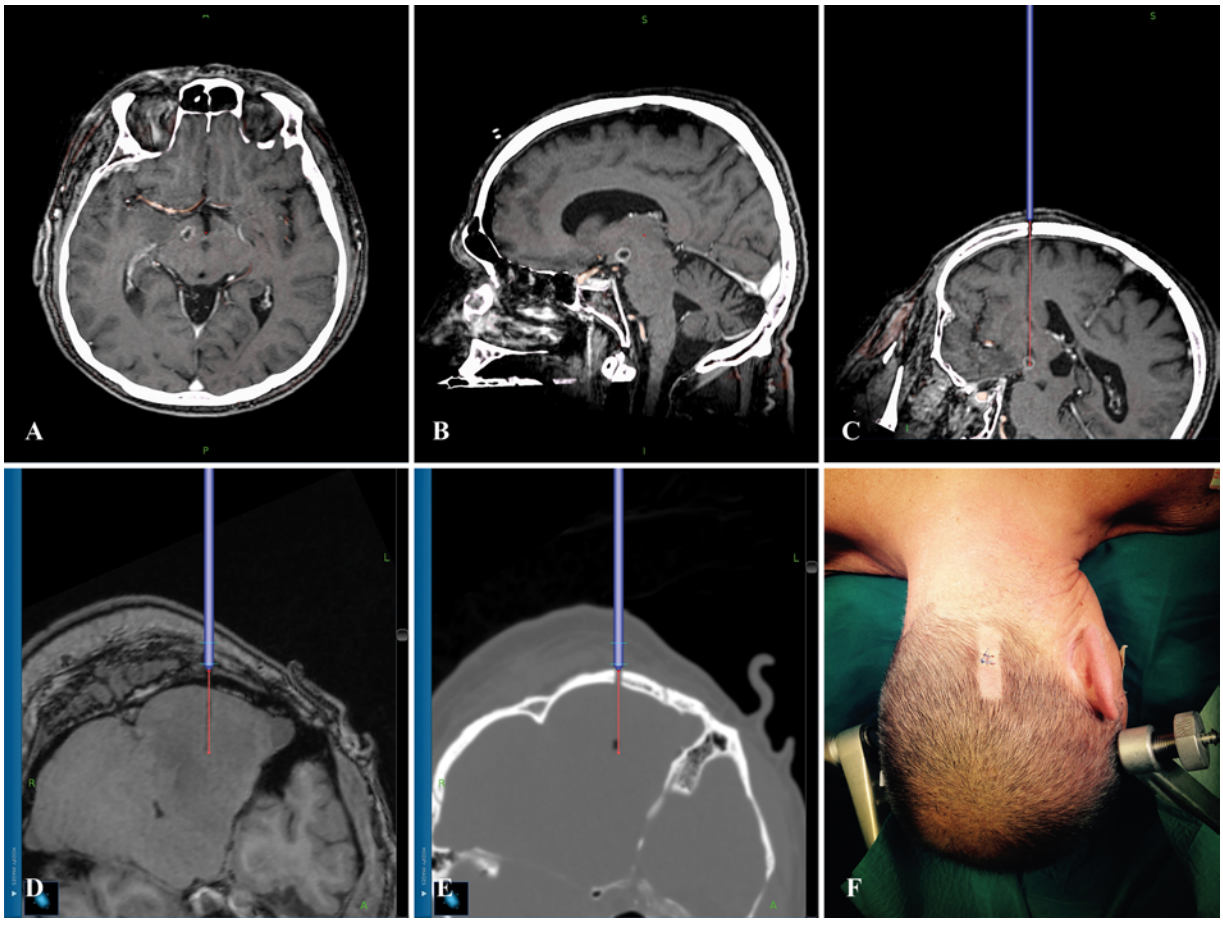

FIG. 3. Illustrative cases. **A–C:** Case of a male patient harboring a WHO grade III oligodendroglioma. Preoperative axial (A) and sagittal (B) contrast-enhanced T1-weighted MR images revealing a left diencephalic lesion with a tumor volume of approximately 0.4 cm^3. The planned biopsy trajectory (*red*) is shown on postoperative T1-weighted MRI images after meticulous preoperative planning (C). The images illustrate the proximity of the biopsy site and trajectory to the left optic tract, the mammillothalamic tract, and vasculature. **D–F:** Case of a male patient with unspecific cerebellar tissue alterations (later confirmed by open resection) illustrating improved cosmesis after a posterior fossa biopsy. Early postoperative T1-weighted MR image (D) and bone-window CT scan (E) revealing the precise location of the overlaid trajectory in the middle of the twist drill burr hole (E) and along the biopsy canal best visible on the postoperative non–contrast-enhanced T1-weighted MR image (D). Due to a significantly shorter skin incision, skin closure with 2 sutures was possible, showing an improved cosmetic result (F).

patient experienced local infection or impaired/prolonged wound healing.

Hemorrhage

We observed 1 case of hemorrhage with a diameter of 38 mm at the target site on postoperative CT scanning (2.9%) using standard robotic guidance, resulting in a transient clinical deterioration only. This hemorrhage rate is comparable to those of previous studies reporting intracranial hemorrhages in 0.3%–9% of the cases.[6,7,14,17,19,20,26]

Limitations and Outlook

This study was designed to evaluate the feasibility of a novel instrument set for robot-guided biopsies prior to its application in routine clinical practice after certification. Therefore, the study lacks comparison to a standard frameless nonrobotic method.

Due to the small stab incision and twist drill hole of this minimally invasive procedure, a possible drawback is the inability to view dura and cortex during electrocautery. Thus, meticulous preoperative planning is mandatory to avoid vascular and other critical anatomical structures.

Multiple targets at different angled trajectories from 1 entry point can only be reached through a standard burr hole. The twist drill hole of the minimally invasive procedure does not allow various angulations of the biopsy needle, and multiple targets are thus only feasible when straight inline. However, such multiple targets at various angles were never needed during the scope of this study.

Conclusions

We present a novel, minimally invasive instrument set for robot-guided stereotactic biopsies. Application was feasible in all cases, and integration into the intraoperative workflow was seamless. According to our data, the use of the minimally invasive robotic guidance procedure

can significantly improve accuracy, reduce operating time, and improve the cosmetic result.

Acknowledgments

We thank Ingrid Dobsak for preparation of the figures.

References

1. Air EL, Leach JL, Warnick RE, McPherson CM: Comparing the risks of frameless stereotactic biopsy in eloquent and noneloquent regions of the brain: a retrospective review of 284 cases. **J Neurosurg 111:**820–824, 2009
2. Barnett GH, Miller DW, Weisenberger J: Frameless stereotaxy with scalp-applied fiducial markers for brain biopsy procedures: experience in 218 cases. **J Neurosurg 91:**569–576, 1999
3. Bernays RL, Kollias SS, Khan N, Brandner S, Meier S, Yonekawa Y: Histological yield, complications, and technological considerations in 114 consecutive frameless stereotactic biopsy procedures aided by open intraoperative magnetic resonance imaging. **J Neurosurg 97:**354–362, 2002
4. Bjartmarz H, Rehncrona S: Comparison of accuracy and precision between frame-based and frameless stereotactic navigation for deep brain stimulation electrode implantation. **Stereotact Funct Neurosurg 85:**235–242, 2007
5. Brinker T, Arango G, Kaminsky J, Samii A, Thorns U, Vorkapic P, et al: An experimental approach to image guided skull base surgery employing a microscope-based neuronavigation system. **Acta Neurochir (Wien) 140:**883–889, 1998
6. Dammers R, Haitsma IK, Schouten JW, Kros JM, Avezaat CJJ, Vincent AJPE: Safety and efficacy of frameless and frame-based intracranial biopsy techniques. **Acta Neurochir (Wien) 150:**23–29, 2008
7. Dammers R, Schouten JW, Haitsma IK, Vincent AJPE, Kros JM, Dirven CMF: Towards improving the safety and diagnostic yield of stereotactic biopsy in a single centre. **Acta Neurochir (Wien) 152:**1915–1921, 2010
8. Dorfer C, Minchev G, Czech T, Stefanits H, Feucht M, Pataraia E, et al: A novel miniature robotic device for frameless implantation of depth electrodes in refractory epilepsy. **J Neurosurg 126:**1622–1628, 2017
9. Dorfer C, Stefanits H, Pataraia E, Wolfsberger S, Feucht M, Baumgartner C, et al: Frameless stereotactic drilling for placement of depth electrodes in refractory epilepsy: operative technique and initial experience. **Neurosurgery 10 (Suppl 4):**582–591, 2014
10. Dorward NL, Paleologos TS, Alberti O, Thomas DGT: The advantages of frameless stereotactic biopsy over frame-based biopsy. **Br J Neurosurg 16:**110–118, 2002
11. Field M, Witham TF, Flickinger JC, Kondziolka D, Lunsford LD: Comprehensive assessment of hemorrhage risks and outcomes after stereotactic brain biopsy. **J Neurosurg 94:**545–551, 2001
12. Golfinos JG, Fitzpatrick BC, Smith LR, Spetzler RF: Clinical use of a frameless stereotactic arm: results of 325 cases. **J Neurosurg 83:**197–205, 1995
13. Gralla J, Nimsky C, Buchfelder M, Fahlbusch R, Ganslandt O: Frameless stereotactic brain biopsy procedures using the Stealth Station: indications, accuracy and results. **Zentralbl Neurochir 64:**166–170, 2003
14. Grossman R, Sadetzki S, Spiegelmann R, Ram Z: Haemorrhagic complications and the incidence of asymptomatic bleeding associated with stereotactic brain biopsies. **Acta Neurochir (Wien) 147:**627–631, 2005
15. Grunert P, Darabi K, Espinosa J, Filippi R: Computer-aided navigation in neurosurgery. **Neurosurg Rev 26:**73–101, 2003
16. Grunert P, Müller-Forell W, Darabi K, Reisch R, Busert C, Hopf N, et al: Basic principles and clinical applications of neuronavigation and intraoperative computed tomography. **Comput Aided Surg 3:**166–173, 1998
17. Kondziolka D, Firlik AD, Lunsford LD: Complications of stereotactic brain surgery. **Neurol Clin 16:**35–54, 1998
18. Kral F, Puschban EJ, Riechelmann H, Pedross F, Freysinger W: Optical and electromagnetic tracking for navigated surgery of the sinuses and frontal skull base. **Rhinology 49:**364–368, 2011
19. Krieger MD, Chandrasoma PT, Zee CS, Apuzzo ML: Role of stereotactic biopsy in the diagnosis and management of brain tumors. **Semin Surg Oncol 14:**13–25, 1998
20. Kulkarni AV, Guha A, Lozano A, Bernstein M: Incidence of silent hemorrhage and delayed deterioration after stereotactic brain biopsy. **J Neurosurg 89:**31–35, 1998
21. Lefranc M, Capel C, Pruvot AS, Fichten A, Desenclos C, Toussaint P, et al: The impact of the reference imaging modality, registration method and intraoperative flat-panel computed tomography on the accuracy of the ROSA® stereotactic robot. **Stereotact Funct Neurosurg 92:**242–250, 2014
22. Lefranc M, Capel C, Pruvot-Occean AS, Fichten A, Desenclos C, Toussaint P, et al: Frameless robotic stereotactic biopsies: a consecutive series of 100 cases. **J Neurosurg 122:**342–352, 2015
23. Louis DN, Perry A, Reifenberger G, von Deimling A, Figarella-Branger D, Cavenee WK, et al: The 2016 World Health Organization Classification of Tumors of the Central Nervous System: a summary. **Acta Neuropathol 131:**803–820, 2016
24. Maurer CR Jr, Aboutanos GB, Dawant BM, Gadamsetty S, Margolin RA, Maciunas RJ, et al: Effect of geometrical distortion correction in MR on image registration accuracy. **J Comput Assist Tomogr 20:**666–679, 1996
25. Maurer CR Jr, Maciunas RJ, Fitzpatrick JM: Registration of head CT images to physical space using a weighted combination of points and surfaces. **IEEE Trans Med Imaging 17:**753–761, 1998
26. McGirt MJ, Woodworth GF, Coon AL, Frazier JM, Amundson E, Garonzik I, et al: Independent predictors of morbidity after image-guided stereotactic brain biopsy: a risk assessment of 270 cases. **J Neurosurg 102:**897–901, 2005
27. Minchev G, Kronreif G, Martínez-Moreno M, Dorfer C, Micko A, Mert A, et al: A novel miniature robotic guidance device for stereotactic neurosurgical interventions: preliminary experience with the iSYS1 robot. **J Neurosurg 126:**985–996, 2017
28. Moriarty TM, Quinones-Hinojosa A, Larson PS, Alexander E III, Gleason PL, Schwartz RB, et al: Frameless stereotactic neurosurgery using intraoperative magnetic resonance imaging: stereotactic brain biopsy. **Neurosurgery 47:**1138–1146, 2000
29. Paleologos TS, Dorward NL, Wadley JP, Thomas DG: Clinical validation of true frameless stereotactic biopsy: analysis of the first 125 consecutive cases. **Neurosurgery 49:**830–837, 2001
30. Pötzi C, Becherer A, Marosi C, Karanikas G, Szabo M, Dudczak R, et al: [11C] methionine and [18F] fluorodeoxyglucose PET in the follow-up of glioblastoma multiforme. **J Neurooncol 84:**305–314, 2007
31. Quiñones-Hinojosa A, Ware ML, Sanai N, McDermott MW: Assessment of image guided accuracy in a skull model: comparison of frameless stereotaxy techniques vs. frame-based localization. **J Neurooncol 76:**65–70, 2006
32. Roessler K, Ungersboeck K, Aichholzer M, Dietrich W, Czech T, Heimberger K, et al: Image-guided neurosurgery comparing a pointer device system with a navigating microscope: a retrospective analysis of 208 cases. **Minim Invasive Neurosurg 41:**53–57, 1998
33. Smith JS, Quiñones-Hinojosa A, Barbaro NM, McDermott MW: Frame-based stereotactic biopsy remains an important

diagnostic tool with distinct advantages over frameless stereotactic biopsy. **J Neurooncol 73:**173–179, 2005
34. Spivak CJ, Pirouzmand F: Comparison of the reliability of brain lesion localization when using traditional and stereotactic image-guided techniques: a prospective study. **J Neurosurg 103:**424–427, 2005
35. Tavares WM, Tustumi F, da Costa Leite C, Gamarra LF, Amaro E Jr, Teixeira MJ, et al: An image correction protocol to reduce distortion for 3-T stereotactic MRI. **Neurosurgery 74:**121–126, n126–n127, 2014
36. Varma TRK, Eldridge P: Use of the NeuroMate stereotactic robot in a frameless mode for functional neurosurgery. **Int J Med Robot 2:**107–113, 2006
37. Widhalm G, Minchev G, Woehrer A, Preusser M, Kiesel B, Furtner J, et al: Strong 5-aminolevulinic acid-induced fluorescence is a novel intraoperative marker for representative tissue samples in stereotactic brain tumor biopsies. **Neurosurg Rev 35:**381–391, 2012
38. Wolfsberger S, Rössler K, Regatschnig R, Ungersböck K: Anatomical landmarks for image registration in frameless stereotactic neuronavigation. **Neurosurg Rev 25:**68–72, 2002

Disclosures

Dr. Wolfsberger: clinical or research support for this study from and an education consultant for Medtronic, and consultant for MGS.

Author Contributions

Conception and design: Wolfsberger, Minchev, Kronreif, Legnani. Acquisition of data: Minchev, Dorfer, Micko, Maschke. Analysis and interpretation of data: Wolfsberger, Minchev. Drafting the article: Wolfsberger, Minchev. Critically revising the article: Wolfsberger, Minchev, Dorfer, Widhalm, Knosp. Reviewed submitted version of manuscript: all authors. Approved the final version of the manuscript on behalf of all authors: Wolfsberger. Statistical analysis: Minchev, Micko. Administrative/technical/material support: Minchev, Kronreif, Ptacek, Dorfer, Knosp. Study supervision: Wolfsberger, Minchev.

Supplemental Information

Previous Presentations

Portions of this work were presented at the 17th European Congress of Neurosurgery, European Association of Neurosurgical Societies, Venice, Italy, October 1–5, 2017.

Correspondence

Stefan Wolfsberger: Medical University of Vienna, Austria. stefan.wolfsberger@meduniwien.ac.at.